

Extended surface exposures of granitoid compositions in Syrtis Major, Mars

Joshua L. Bandfield¹

Received 23 December 2005; revised 16 February 2006; accepted 22 February 2006; published 31 March 2006.

[1] The number of quartz and feldspar rich surfaces identified in northwestern Syrtis Major has been extended beyond previously reported results to a region of about 230 by 125 km. Thermal Emission Imaging System infrared data were used to locate surfaces spectrally identical to previously reported central peak units in Syrtis Major. These surfaces are indicative of the production of highly differentiated magmas. Though it is possible that the granitoid exposures add to the variety of igneous compositions associated with the Syrtis Major volcanic construct, the geologic context of these exposures suggests a formation that predates Syrtis Major. **Citation:** Bandfield, J. L. (2006), Extended surface exposures of granitoid compositions in Syrtis Major, Mars, *Geophys. Res. Lett.*, *33*, L06203, doi:10.1029/2005GL025559.

1. Introduction

[2] A variety of igneous compositions are present on Mars. Martian Meteorites and remote sensing indicate that much of the crust may be composed of mafic compositions [e.g., *Singer et al.*, 1979; *McSween*, 1994; *Mustard et al.*, 1997, 2005; *Bandfield et al.*, 2000a; *Christensen et al.*, 2001, 2005; *Bibring et al.*, 2005]. However, there is evidence for a variety of igneous lithologies, including low, moderate, and high silica compositions [*Bandfield et al.*, 2000a; *Hoefen et al.*, 2003; *Hamilton et al.*, 2003; *Bandfield et al.*, 2004a; *Christensen et al.*, 2005]. Production of this variety of compositions requires igneous mechanisms beyond simple partial melting of mantle material that is assumed to produce basaltic compositions on terrestrial planets [*Basaltic Volcanism Study Project*, 1981].

[3] Orbital spectroscopy has provided both geologic context and extensive coverage of the Martian surface with respect to exposed igneous compositions. Visible through thermal infrared (TIR) wavelength spectral measurements have provided highly complimentary information about the mineralogy of the Martian surface. TIR measurements from the Thermal Emission Spectrometer (TES) and the Thermal Emission Imaging System (THEMIS) onboard the Mars Global Surveyor and Mars Odyssey spacecraft respectively have provided information about the bulk surface compositions [e.g., *Christensen et al.*, 2001; *Bandfield et al.*, 2000b; *Hoefen et al.*, 2003; *Bandfield et al.*, 2004a; *Hamilton and Christensen*, 2005; *Christensen et al.*, 2005]. Near-infrared measurements from the Imaging Spectrometer for Mars (ISM), the Observatoire pour la

Minéralogie, l'Eau, les Glaces, et l'Activité (OMEGA), and previous telescopic measurements have provided information about the primary igneous mineralogy from ~ 1 and $2 \mu\text{m}$ Fe^{2+} absorptions. On Mars, these absorptions are dominated by pyroxenes and olivines [e.g., *Singer et al.*, 1979; *Mustard et al.*, 1997, 2005; *Bibring et al.*, 2005].

[4] TES and THEMIS data have been used to identify Martian surface compositions dominated by quartz and plagioclase feldspar [*Bandfield et al.*, 2004a]. The initial identification of these materials was near the central peaks of two craters ~ 95 km apart in northern Syrtis Major. The work presented here shows that these materials are more extensive than initially reported and that the exposures are not necessarily associated with the cratering process.

2. Data and Methods

[5] The TIR imager on THEMIS consists of a 320 by 240 element uncooled microbolometer array with 9 spectral channels centered at wavelengths between 9 and $15 \mu\text{m}$. Spatial sampling is 100 m from the ~ 420 km altitude circular Mars Odyssey spacecraft orbit. *Christensen et al.* [2004] and *Bandfield et al.* [2004b] present detailed descriptions of calibration methods and radiometric uncertainties.

[6] For the targets presently described, only TIR imagery was available at the time of this study. Daytime band 9 ($12.2 \mu\text{m}$) radiance images were used for determination of local and regional morphology. Surface composition is determined using THEMIS bands 1 through 9 at 8 wavelengths between 6.3 and $12.2 \mu\text{m}$. All images presented here for determination of surface composition have average surface temperatures of 240 to 255 K. Thermal inertia values were obtained using THEMIS band 9 night time brightness temperature images using a method similar to that of *Ferguson et al.* [2006].

[7] The methods that were used in this study are described in detail by *Bandfield et al.* [2004a, 2004b]. Decorrelation stretch (DCS) [*Gillespie et al.*, 1986] THEMIS radiance images were used as the primary means for detecting the possible presence of granitoid composition surfaces. All warm surface (average temperature >220 K) infrared images from the entire THEMIS data set have been processed into three multiple band combination DCS and combined with the corresponding surface temperature image (referred to as 4-panel images below) [*Bandfield et al.*, 2004a]. This method allows for a rapid assessment of spectral variability within an image and can be interpreted in a manner similar to other terrestrial imaging TIR remote sensing studies [e.g., *Gillespie*, 1992; *Ramsey et al.*, 1999].

[8] Data used for this study were corrected for atmospheric effects by using the constant radiance offset correction and surface emissivity retrieval algorithms of *Bandfield*

¹Department of Geological Sciences, Arizona State University, Tempe, Arizona, USA.

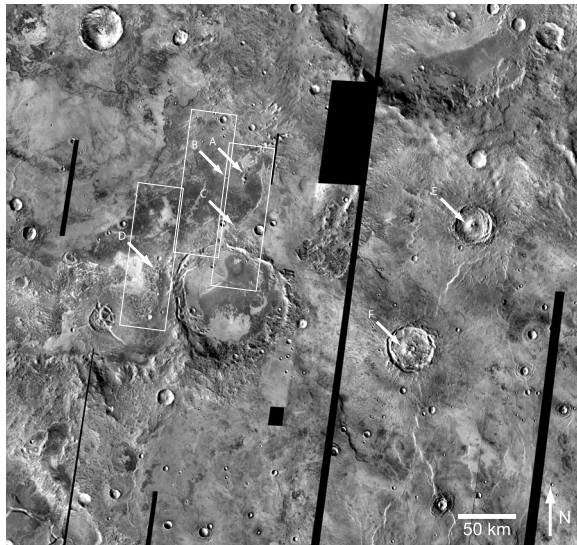


Figure 1. Mosaic of THEMIS band 9 radiance images. Arrows denote approximate locations of quartzofeldspathic surfaces and boxes indicate the areas covered by images shown in Figure 2. Letters correspond to the following locations: A. Large knobby terrain B. Small knobby terrain C. Eastern fractured terrain D. Western fractured terrain E. North crater F. South crater. The mosaic covers approximately 60.1 to 67.2 E and 16.3 to 22.5 N.

et al. [2004b]. In addition, individual THEMIS pixels can be deconvolved using a set of endmember spectra to create spectral unit concentration maps [e.g., *Adams et al.*, 1986; *Gillespie*, 1992; *Ramsey et al.*, 1999; *Bandfield et al.*, 2004a, 2004b]. A linear least-squares fit of end-members to THEMIS pixels is performed and the concentrations and RMS error between measured and modeled spectra are retrieved. For this study, end-members were selected from both TES data and laboratory spectra convolved to the THEMIS spectral band passes in manner similar to that of *Bandfield et al.* [2004a, 2004b].

3. Results

[9] Surfaces of interest were initially identified near the central peaks of two craters in northern Syrtis Major by examining individual 4-panel DCS images (not shown here). Regional coverage of TIR THEMIS data warm enough for spectral examination was nearly 100% at the time of this study (Figure 1), which allowed for the identification of additional exposures of similar high silica surfaces (Figure 2). The emissivity of these surfaces is lower near 8.5 μm (band 4) and higher from ~ 10 –12 μm (bands 6–8, Figure 3) than the surrounding basaltic/basaltic andesite plains [*Bandfield*, 2002; *Ruff*, 2003; *Christensen et al.*, 2005]. Surfaces with this spectral signature appear as yellow, yellow, and magenta in the bands 8-7-5, 9-6-4, and 6-4-2 DCS images respectively.

[10] Four separate exposures were identified near the southwest rim of Antoniadi crater (Figure 1). Two of the exposures occur in knobby terrains that are surrounded by the relatively flat surface of the crater interior. The other two exposures are located in two areas of heavily fractured terrain that lie near the boundary between the southeast

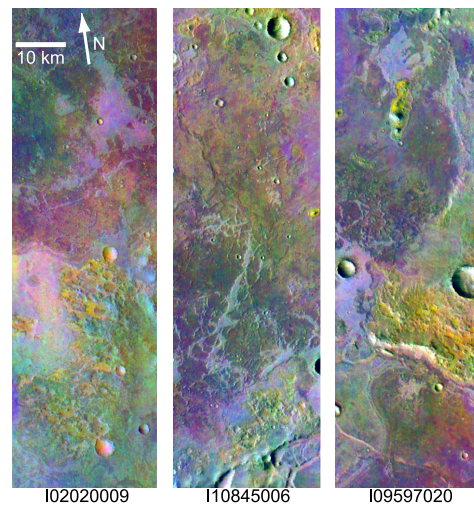


Figure 2. Decorrelation stretch THEMIS images. Bands 8, 7, and 5 were projected as red, green, and blue respectively. Yellow colors coincide with higher band 8 and 7 and lower band 5 emissivities, consistent with surfaces that contain quartz and feldspar.

rim of Antoniadi crater and an unnamed 75 km diameter crater. These exposures coincide with lower elevations in the region, but are relatively isolated and not ubiquitous. The spectrally unique exposures are within 61.8–65.9 E longitude and 18.4–20.5 N latitude; these coordinates cover a region of roughly 230 by 125 km. The total areal extent of exposures with concentrations above 0.2 (discussed below) is 19 km^2 . A careful examination of THEMIS images within the region found no additional exposures.

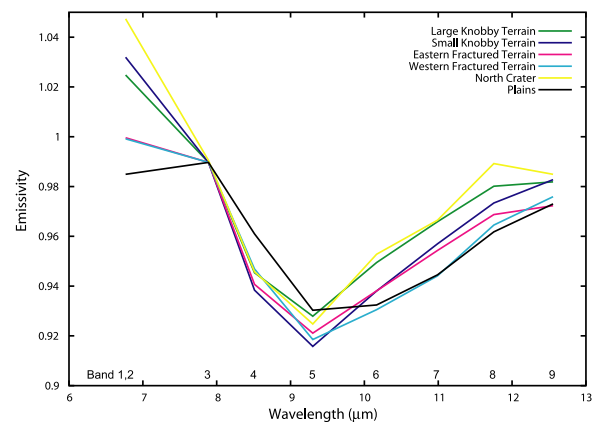


Figure 3. THEMIS surface emissivity spectra from surfaces exposed in the images shown in Figure 2. Basaltic plains (black) have higher emissivity in THEMIS bands 4 and 5 and lower emissivity in bands 6–8 relative to the quartz and feldspar rich surfaces (knobs, fractured terrains, and crater). The north crater spectrum is taken from the previously published central peak unit exposure [*Bandfield et al.*, 2004a]. Emissivities are above unity for many of these spectra because band 3 was used for surface temperature estimation even though there is lower emissivity at these wavelengths relative to bands 1/2 for quartz-rich surfaces.

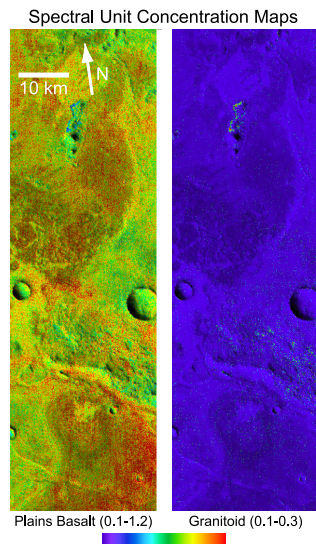


Figure 4. Spectral unit end-member plains basalt and quartz monzonite concentration maps for THEMIS image I09597020. Colors are draped over grayscale band 9 radiance images for context.

[11] The atmospherically corrected surface spectra of the spectrally unique exposures are similar to those previously identified in the central peaks of two craters to the east [Bandfield *et al.*, 2004a] (Figure 3). All exposures have absorptions concentrated at shorter wavelengths than the surrounding plains. All of the exposures also have higher $\sim 6.8 \mu\text{m}$ (bands 1/2) emissivity than the surrounding plains, indicating that there is some absorption at $8 \mu\text{m}$ (band 3) relative to the plains. Some of the $6.8 \mu\text{m}$ emissivity variation is due to increased noise at these wavelengths, however. The surface spectra from the western fractured terrain do not appear as prominent as the other exposures.

[12] Spectral unit concentration maps were produced by deconvolving bands 3 through 9 of each pixel of the atmospherically corrected data using the regional Mars surface spectrum derived from TES data, a laboratory spectrum of quartz monzonite, a water ice cloud spectral shape [Bandfield *et al.*, 2000b], and a blackbody spectrum (Figure 4) [Bandfield *et al.*, 2004b]. Average RMS errors between measured and modeled spectra are 0.0027, 0.0033, and 0.0033 for THEMIS images I02020009, I09597020, and I10845006 respectively. RMS errors are anti-correlated with surface temperature and are primarily due to random noise. This indicates that no additional spectral end-members are necessary to model the data.

[13] Retrieved concentrations of the quartz monzonite spectral end-member are highest in the eastern knobby and fractured terrains (up to 0.4) with lower concentrations in the western knobby terrain (0.3) and western fractured terrain (0.17). The regional Mars surface end-member concentrations are anti-correlated with the quartz monzonite, ranging from ~ 0.2 – 1.0 for quartz monzonite concentrations of 0.4 – 0 respectively.

4. Discussion

[14] Three of the four granitoid composition surface units are identical within uncertainties to the exposures near the

central peaks of craters to the east (Figure 3). The regional proximity of these surface units to the previously reported central peak exposures implies that they share a similar formation history and may be part of a single lithologic unit. The western fractured terrain exposure is not as prominent as the other exposures and appears to have a significant amount of the plains spectral signature contributing to its emissivity. However, it does have the same spectral trends as the other exposures and occurs in a similar surface morphology as the eastern fractured terrain exposure.

[15] Concentrations of the spectral endmembers from the deconvolution are highly dependent on spectral contrast. The quartz monzonite end-member has relatively low concentrations even where the plains unit concentrations are near zero. This is likely due to the relatively high spectral contrast of the quartz monzonite endmember, which comes from a laboratory spectrum of a rock sample. Nighttime THEMIS temperature data in the region are consistent with particulate surfaces rather than bedrock exposures. Particulate surfaces have roughly half the spectral contrast of broken rock surfaces [Ruff, 1998]. Consequently, the areal coverage of the quartz monzonite endmember is roughly double the unit map concentrations (up to 70–80%), consistent with the coincident low plains unit concentrations (0–20%).

[16] Unfortunately, three of the four additional exposures are either too small or too diffuse to be detectable with the higher spectral resolution but lower spatial resolution TES data. In the case of the larger knobby terrain and rough terrain exposures, there is no warm surface coverage of TES data. As a result, the only source of specific mineralogy from TES data remains the northern crater central peak exposure [Bandfield *et al.*, 2004a]. Both TES and THEMIS data are consistent with lithologies dominated by quartz and plagioclase feldspar, such as granitoids.

[17] The granitoid composition surfaces cover a significantly larger region than the two previously identified central peak exposures. Though thermal inertia values indicate that the surfaces are likely composed of loose particulate material, the association of granitoid surfaces with specific surface features and their localized nature suggest that the material has not been transported a significant distance from its source. It is impossible to determine if this composition is continuous in the subsurface where it is not exposed or how much more extensive it may be. There are few surface features of similar morphology (e.g., central peak craters of similar size) as those that coincide with the exposures of quartz and feldspar rich surfaces within the region. It may be a continuous unit within the Martian subsurface, especially as the composition and context of the exposures suggest a subsurface formation. If the granitoid composition is not extensive at depth then it would be remarkable that it is largely confined to the localities that happen to be exposed. However, rock unit distributions can be more complex than a simple continuous body.

[18] Syrtis Major is the only major volcanic construct on Mars that is not mantled with obscuring dust. This has enabled orbital remote sensing to gain insight into the variety of igneous compositions present at the surface in the region [Mustard *et al.*, 1997; Bandfield, 2002; Hoefen *et al.*, 2003; Bandfield *et al.*, 2004a; Hamilton

and Christensen, 2005; Christensen *et al.*, 2005]. The granitoid composition may be part of the ancient Noachian crust and could predate Syrtis Major, however. Antoniadi crater has been resurfaced by Hesperian age lava flows from Syrtis Major [Hiesinger and Head, 2004]. The granitoid compositions had to be present and exposed prior to this resurfacing event. This association may disassociate the granitoid exposures from the Syrtis Major construct.

[19] It is difficult to postulate on what the formation mechanisms may be outside the paradigm of plate tectonics, which is the dominant factor for producing differentiated magma compositions on Earth. However, large quantities of granitoid rocks were produced as trondhjemites on Earth by partial melting near the base of thick sequences of basaltic crust at 2.8 to 3.8 Ga, prior to the establishment of modern plate tectonics [Barker, 1979]. Though such a formation mechanism is plausible on Mars, there is little evidence available at this time to either support or refute it [Bandfield *et al.*, 2004a].

5. Conclusions

[20] Identified quartzofeldspathic surfaces in northwestern Syrtis Major have been extended beyond previously reported results to a region about 230 by 125 km. While it is impossible from the existing data to determine the extent of any alteration, these surfaces indicate that there are mechanisms on Mars that produce highly differentiated magmas. Though it is possible that the granitoid exposures add to the variety of igneous compositions associated with the Syrtis Major volcanic construct, the geologic context of these exposures suggests a formation that predates Syrtis Major.

[21] **Acknowledgments.** Thanks to L. Cherednik, A. Dombovari, and K. Bender for collecting excellent THEMIS observations. P. Christensen, G. Mehall, C. Edwards, K. Murray, K. Nowicki, N. Gorelick, and M. Weiss-Malik provided essential support for THEMIS. THEMIS is on the Mars Odyssey, which is operated by many dedicated folks at JPL and Lockheed Martin. Thanks also to J. Moersch and an anonymous reviewer for excellent suggestions that significantly improved this manuscript.

References

- Adams, J. B., M. O. Smith, and P. E. Johnson (1986), Spectral mixture modeling—A new analysis of rock and soil types at the Viking Lander 1 site, *J. Geophys. Res.*, *91*, 8098–8112.
- Bandfield, J. L. (2002), Global mineral distributions on Mars, *J. Geophys. Res.*, *107*(E6), 5042, doi:10.1029/2001JE001510.
- Bandfield, J. L., V. E. Hamilton, and P. R. Christensen (2000a), A global view of Martian Surface compositions from MGS-TES, *Science*, *287*, 1626–1630.
- Bandfield, J. L., P. R. Christensen, and M. D. Smith (2000b), Spectral dataset factor analysis and endmember recovery: Application to Martian atmospheric particulates, *J. Geophys. Res.*, *105*, 9573–9588.
- Bandfield, J. L., V. E. Hamilton, P. R. Christensen, and H. Y. McSweeney Jr. (2004a), Identification of quartzofeldspathic materials on Mars, *J. Geophys. Res.*, *109*, E10009, doi:10.1029/2004JE002290.
- Bandfield, J. L., D. Rogers, M. D. Smith, and P. R. Christensen (2004b), Atmospheric correction and surface spectral unit mapping using Thermal Emission Imaging System data, *J. Geophys. Res.*, *109*, E10008, doi:10.1029/2004JE002289.
- Barker, F. (1979), Trondhjemite: Definition, environment and hypothesis of origin, in *Trondhjemites, Dacites, and Related Rocks*, edited by F. Barker, pp. 1–12, Elsevier, New York.
- Basaltic Volcanism Study Project (1981), *Basaltic Volcanism on the Terrestrial Planets*, 1286 pp., Elsevier, New York.
- Bibring, J.-P., *et al.* (2005), Mars surface diversity as revealed by the OMEGA/Mars express observations, *Science*, *307*, 1576–1581.
- Christensen, P. R., *et al.* (2001), The Mars Global Surveyor Thermal Emission Spectrometer experiment: Investigation description and surface science results, *J. Geophys. Res.*, *106*, 23,823–23,871.
- Christensen, P. R., *et al.* (2004), The Thermal Emission Imaging System (THEMIS) for the Mars 2001 Odyssey mission, *Space Sci. Rev.*, *110*, 85–130.
- Christensen, P. R., *et al.* (2005), Evidence for magmatic evolution and diversity on Mars from infrared observations, *Nature*, *436*, 504–509.
- Fergason, R. L., P. R. Christensen, J. F. Bell III, M. P. Golombek, K. E. Herkenhoff, and H. H. Kieffer (2006), Physical properties of the Mars Exploration Rover landing sites as inferred from Mini-TES–derived thermal inertia, *J. Geophys. Res.*, *111*, E02S21, doi:10.1029/2005JE002583.
- Gillespie, A. R. (1992), Spectral mixture analysis of multispectral thermal infrared images, *Remote Sens. Environ.*, *42*, 137–145.
- Gillespie, A. R., A. B. Kahle, and R. E. Walker (1986), Color enhancement of highly correlated images: I. Decorrelation and HIS contrast stretches, *Remote Sens. Environ.*, *20*, 209–235.
- Hamilton, V. E., and P. R. Christensen (2005), Evidence for extensive, olivine-rich bedrock on Mars, *Geology*, *33*, 433–436.
- Hamilton, V. E., P. R. Christensen, H. Y. McSweeney Jr., and J. L. Bandfield (2003), Searching for the source regions of Martian meteorites using MGS TES: Integrating Martian meteorites into the global distribution of volcanic materials on Mars, *Meteorol. Planet. Sci.*, *38*, 871–886.
- Hiesinger, H., and J. W. Head III (2004), The Syrtis Major volcanic province, Mars: Synthesis from Mars Global Surveyor data, *J. Geophys. Res.*, *109*, E01004, doi:10.1029/2003JE002143.
- Hoefen, T. M., R. N. Clark, J. L. Bandfield, M. D. Smith, J. C. Pearl, and P. R. Christensen (2003), Discovery of Olivine in the Nili Fossae Region of Mars, *Science*, *302*, 627–630.
- McSweeney, H. Y., Jr. (1994), What have we learned about Mars from SNC meteorites, *Meteoritics*, *29*, 757–779.
- Mustard, J. F., S. Murchie, S. Erard, and J. Sunshine (1997), In situ compositions of Martian volcanics: Implications for the mantle, *J. Geophys. Res.*, *102*, 25,605–25,616.
- Mustard, J. F., F. Poulet, A. Gendrin, J.-P. Bibring, Y. Langevin, B. Gondet, N. Mangold, G. Bellucci, and F. Altieri (2005), Olivine and pyroxene diversity in the crust of Mars, *Science*, *307*, 1594–1597.
- Ramsey, M. S., P. R. Christensen, N. Lancaster, and D. A. Howard (1999), Identification of sand sources and transport pathways at Kelso Dunes, California using thermal infrared remote sensing, *Geol. Soc. Am. Bull.*, *111*, 636–662.
- Ruff, S. W. (1998), Quantitative thermal infrared emission spectroscopy applied to granitoid petrology, Ph.D. diss., 234 pp., Arizona State Univ., Tempe.
- Ruff, S. W. (2003), An emerging picture of the volcanic history of Syrtis Major from multiple dataset views, *Eos Trans. AGU*, *84*(46), Fall Meet. Suppl., Abstract P12C-03.
- Singer, R. B., T. B. McCord, R. N. Clark, J. B. Adams, and R. L. Huguenin (1979), Mars surface composition from reflection spectroscopy: A summary, *J. Geophys. Res.*, *84*, 8415–8425.

J. L. Bandfield, Department of Geological Sciences, Arizona State University, Tempe, AZ 85287–6305, USA. (joshua.bandfield@asu.edu)